Journal of Engineering Research and Reports

Volume 26, Issue 5, Page 66-75, 2024; Article no.JERR.115216
ISSN: 2582-2926

Multi-feature Learning Adaptive Network for Underwater Image Enhancement

Qingzheng Wang [a], Bin Li [a*] and Xixi Zhu [a]

[a] *North China University of Water Resources and Electric Power, School of Information Engineering, China.*

Authors' contributions

This work was carried out in collaboration among all authors. All authors read and approved the final manuscript.

Article Information

DOI: 10.9734/JERR/2024/v26i51135

Open Peer Review History:
This journal follows the Advanced Open Peer Review policy. Identity of the Reviewers, Editor(s) and additional Reviewers, peer review comments, different versions of the manuscript, comments of the editors, etc are available here: https://www.sdiarticle5.com/review-history/115216

Original Research Article

Received: 24/01/2024
Accepted: 28/03/2024
Published: 03/04/2024

ABSTRACT

Underwater image enhancement faces variety of challenges owing to the diversity of underwater scenes (viewed as water types) and the rich multi-frequency information. To deal with these challenges, this paper proposes a multi-feature learning adaptive underwater image enhancement network comprising an adaptive module and a dual-layer synchronous enhancement network. First, we design an adaptive module which enables the determination of water type inside the model and eliminates the negative effect of water type diversity by building water type related features. Then, the model learns high-frequency and low-frequency features through a dual-layer synchronous enhancement network to extract more comprehensive information. Finally, the outputs of the dual-layer network are merged to obtain more realistic underwater enhanced images. Numerous experiments have shown that the proposed method outperforms the comparison method for visual perception and assessment metrics.

**Corresponding author: Email: lb18237387633@163.com;*

Keywords: Underwater image; image enhancement; deep learning; multi-frequency information.

1. INTRODUCTION

Underwater imagery is an important tool for obtaining marine information and plays an essential role in the field of marine research and underwater robotics. However, the light suffers severe attenuation and scattering during it propagates underwater. Complex underwater imaging processes lead to low contrast, color distortion and blurred details in underwater images. Besides, different underwater scenes, namely water types, have different effects on degraded images. However, many existing studies on underwater image enhancement have not specifically focused on addressing the effects of different water types. In addition, underwater images contain rich information that can be simply divided into low-frequency and high-frequency components. High-frequency components refer to local information, mainly consisting of texture and noise details in the image. Conversely, low-frequency components mainly contain global information within the color and structure.

In this paper, we propose a multi-feature learning adaptive underwater image enhancement network to solve the effects of different water types and multi-frequency features on underwater image enhancement. The proposed network primarily comprises two parts: an adaptive module and a dual-layer synchronous enhancement network. The adaptive module is able to adaptively cope with the interference caused by different water types to the degraded images, preserving the features relevant to the scene. The network employs two branches to learn high-frequency and low-frequency features, integrating attention operation [1] with different receptive fields to ensure synchronized extraction of local features and modeling of long-term dependencies for enhanced image quality. This method allows for a more nuanced analysis of the image content, and makes the color and detail of the enhanced result closer to ground truth, compared with the previous model.

2. RELATED WORK

At present, underwater image enhancement methods can be divided into underwater image enhancement and underwater image restoration depending on the way in which the image is processed underwater.

2.1 Underwater Image Enhancement Method

The underwater image enhancement method does not need to consider the image formation process, and directly processes the pixels of the underwater image to improve visual perception. Jamadandi et al. [2] proposed a deep learning structure based on Wavelet correction transformation. By using Wavelet correction transformation structure, image enhancement is regarded as a problem of image style transformation. Islam et al. [3] formulated the problem as image-to-image conversion, and conducted confrontational training on a large number of data sets based on the GAN model to learn the mapping. Li et al. [4] proposed water-NET to maintain degraded image features and obtain enhanced images by taking histogram equalization, white balance, and gamma correction into account. Uplavikar et al. [5] made an attempt to confirm water type, and learned the features of images by separating unnecessary interference with water types. However, the network structure pays more attention to the characteristic information. Meanwhile, the obtained water type is often inaccurate. Thus, the network tends to introduce color distortion around the edges. Recently, Transformer shines in the field of computer vision.Peng et al. [6] introduced the Transformer model into the task of underwater image enhancement, and combined CNN with Transformer, which can not only model long-term dependence relationships but also pay attention to local information. zhou et al. [7] effectively solved the problems of poor visibility and feature drift of underwater images through a multi-interval sub-histogram perspective equalization underwater image enhancement method, which significantly improved the visual effect and performance of underwater images.

The aboved researches typically employed a single-branch network to enhcane the destoryed image. This structure leads to information disorder when handling various semantic information, resulting in weaknesses in processing multi-frequency information. To address this issue, we introduce a dual-branch synchronous enhancement network where two branches independently decode information of

different frequencies to enhance the model's capacity in extracting multi-frequency information.

2.2 Underwater Image Restoration Method

The purpose of the image restoration method is to solve the serious degradation of the underwater image caused by the scattering of underwater light, other complex underwater imaging environments, such as low contrast, color decay and distortion [8] Chongyi et al. [9] propose a deep underwater image restoration model combined with the attention mechanism, integrating the characteristics of the different color spaces, to solve the underwater image color deviation and the problem of low contrast. John et al. [10] proposed wavelength compensation and image de-fog algorithm (WCID). This model considers removing light scattering and color change caused by the possible artificial light source, and compensating for the difference in wavelength attenuation when crossing water depth to the top of the image. Thus, it can eliminate the distortion caused by light scattering and color change. Since attenuation caused by wavelength changes leads to asymmetric propagation of colors, Prasen Sharma et al. [11] proposed to select corresponding receptive fields based on channel propagation range to suppress irrelevant semantic features, and improve model performance. According to the characteristics of underwater imaging, Drews [12] proposed underwater dark channel Prior (UDCP) to correct background light by combining dark channel Prior (DCP) [13] with color saturation. DCP is used to process ground images, but it has almost no effect on underwater images. UDCP cannot correctly restore scenes of underwater images. Anwar et al. [14] synthesized ten different types of underwater images for training according to the light attenuation coefficients of red, green, and blue in water with the different depths. The underwater image restoration method takes into account different imaging characteristics, but it is hard to calculate too many imaging parameters. Zhou et al. [15] proposed multicolor components and light attenuation (MCLA), which utilizes adaptive background light estimation, depth-map enhancement, and transmission map computation to effectively restore color, detail, and visibility in underwater images. Hou et al. [16] introduced the illumination channel sparsity prior (ICSP) guided variational framework for non-uniform illumination underwater image restoration, leveraging the illumination channel sparsity prior and a variational model with L0 norm term, constraint term, and gradient term to enhance the quality of images.

Although the above methods demonstrate good performance in certain scenarios, they require redesign when confronted with new situations. To enhance the model's generalization, we introduce an adaptive module to assess the water type within the input image and enhance underwater images within a specific domain.

Our proposed model is able to deal well with the impacts of different water types and capture more comprehensive information, achieving state-of-the-art results on real-world [4] [9] [10] and synthetic datasets [17].

3. METHODS

The proposed multi-feature learning adaptive underwater image enhancement framework is shown in Fig.1, the framework consists of two parts, adaptive module to remove the influence of water type on the generated images, and dual-layer synchronous enhancement network to learn features of different frequencies.

3.1 Adaptive Module

The quality of underwater images is degraded due to wavelength-dependent light absorption and scattering in underwater scenes. Besides, underwater images captured from different domain scenes vary in brightness, contrast and visibility. It is difficult to accurately enhance underwater images from different underwater scenes using traditional networks. Hence, we expect our model could recognize the difference information of underwater images, so that the model can be more targeted to reconstruct clear images in specific water types. To address this problem, we propose an adaptive module (AM), which consists of water type classifier and water type related feature extractor, as shown in Figure 1 (b). Next, we will carefully describe each component.

As shown in Fig. 1 (a), The encoder adopts the degraded image as input to obtain the compression encoded features. Although the encoded features contain most of the feature information in an underwater image, the information related to the water types is not sufficient and may lead to erroneous enhancements during processing of the image. Therefore, we apply the encoded feature as the

input of adaptive module to further extract the water type related information. The water type classifier identifies the water type based on the encoded feature. As shown in Fig. 1 (c), the water type classifier consists of convolutional layer, batch normalization, ReLU activation function and linear layer. This structure effectively improves the performance of the model and reduces the computational cost. The water type classifier can be defined as followed:

$$I, I' = C(E(X)) \tag{1}$$

where X is the input image, $C(\cdot)$ and $E(\cdot)$ denote the water type classifier and encoder. I is used to determine the water type of the input image, and I' is the output of the middle layer of the classifier.

Since the encoded features lack sufficient features related to the water type, which leads to disordered information in the decoding process. Thus, we add a water type related feature extractor to get the information related to water type by combine the encoded feature and I'. Specifically, the output of the middle layer of the classifier contains information related to the water type, we employ deconvolutional implementation to upsample it. The upsampled features mostly contain water type information and are weakly correlated with other semantic information in the image. Hence, we perform an element-wise addition operation on the middle layer features and the encoded features, and then use point-wise convolution to obtain water type related features. This process can be defined as follows:

$$\bar{I} = Conv_{1\times1}(DeConv(I')E(X)) \tag{2}$$

where $DeConv(\cdot)$ and $Conv_{1\times1}(\cdot)$ denote deconvolutional layer and point-wise convolution, both of them are followed by batch normalization and ReLU activation function. $\bar{I}$ is the water type related feature, which used as the input of the subsequent dual-layer synchronous enhancement network.

Through this module, it can adaptively remove the influence on the reconstructed image caused by the diversity of water types in the degraded image with different watercolors, and enhanced the generalization ability of the model.

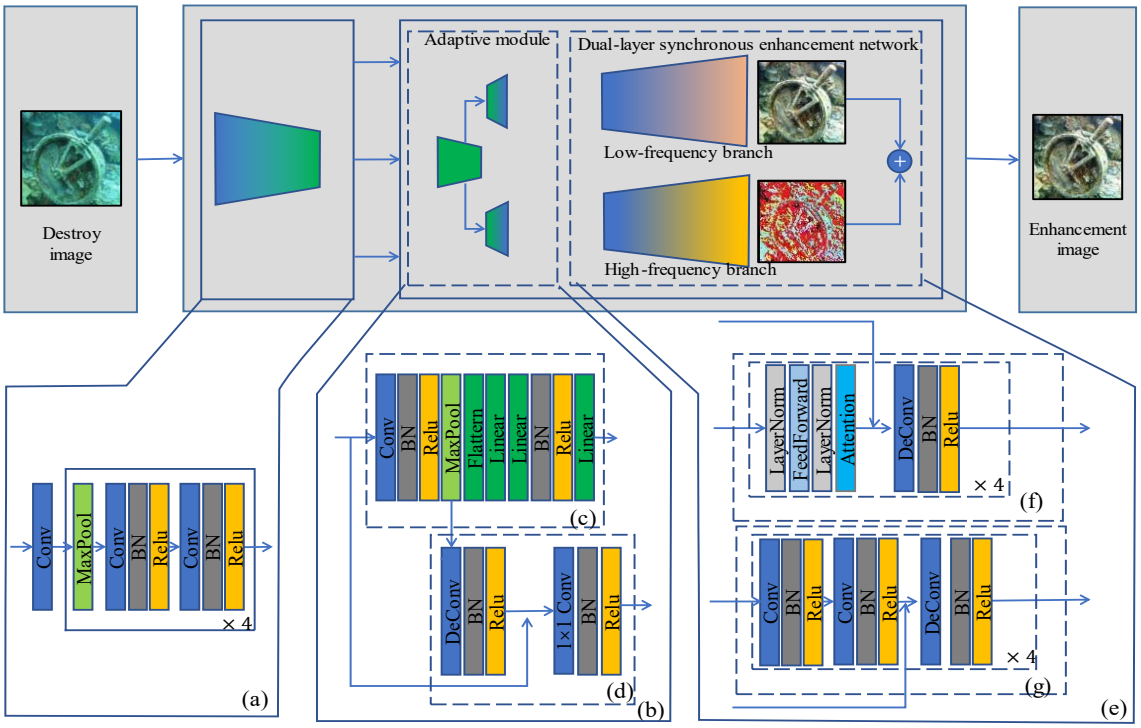

Fig. 1. The framework consists of three parts: (a) the encoder consists of a series of convolutional blocks; (b) an adaptive module consists of (c) water type classifier and (d) water type related feature extractor, which be used to separate the interference of water types; (e) a dual-layer synchronization network consists of (f) low-frequency branch and (g) high-frequency branch for learning high-frequency and low-frequency information separately

3.2 Dual-Layer Synchronous Enhancement Network

Most of the traditional underwater image enhancement networks do not consider the feature information at different frequencies underwater, resulting in enhanced images that still have detail loss. Underwater images are rich in feature information, and features of different frequencies contribute differently to the enhanced images.

Underwater images mainly contain high-frequency information with obvious changes of detailed features such as line and noise, and low-frequency information such as color and texture. In order to learn these features more comprehensively, we propose a dual-layer synchronous enhancement network. The proposed dual-layer synchronous enhancement network is composed of two identical layers, high-frequency branch (HF Branch) and low-frequency branch (LF Branch) and its structure is shown in Fig. 1 (e). The two identical branches with different respective fields to generate high-frequency and low-frequency images. The complex imaging environment of underwater images leads to blurred edges of underwater images and generates a lot of noise. Therefore, we use high-frequency branch which implemented by convolution to reconstruct local detail information. The base feature extract block of the high-frequency branch can be represented as follows:

$$X_i^{\mathrm{H}} = \mathrm{DeConv}(Concat(\mathrm{Conv}_2(\mathrm{Conv}_1((X_{i-1}\hat{}))), \bar{X}_{i-1})) \quad (3)$$

where i is the number of layers of high-frequency branch, and X_0 is the water type related feature, and $\bar{X}_{i-1} = \bar{I}$ when $i = 1$. $\mathrm{Conv}(\cdot)$ denotes convolutional followed by batch normalization and ReLU activation function. Additionally, the feature maps are too coarse to provide more accurate detail information due to multiple downsampling. Therefore, we incorporate skip connections $Concat(\cdot)$ between the corresponding sampling levels to facilitate easier model training. This branch helps the model remove noise while enhancing the sharpness of the edges in the enhanced results.

Morever, due to the effects of underwater light refraction and scattering, a large amount of energy is lost when the light is transmitted to the camera, resulted in color shift and structure blurred global information destroyed during imaging Although CNN is good at processing images, it is weak at long-range modeling of features. Fortunately, it has been recently shown that global attention in Multi-headed Selfattention in Transfromer can effectively capture low-frequency information [18]. Hence, we use low-frequency branch embedded with attention operation to learn global information, as shown in Fig. 1 (f). The base feature extract block of the low-frequency branch can be represented as follows:

$$LF_i(X_{i-1}) = DeConv(Concat(Att(LN(FFD(LN((X_{i-1})))), \bar{X}_{i-1}) \quad (4)$$

Where $LN(\cdot)$ and $FFD(\cdot)$ denote layer normalization and feed forward network, and $Att(\cdot)$ represents attention operation. This branch further enhances the similarity between each color space of the output image and ground truth.

The dual-layer synchronous enhancement network is capable of learning information at different frequencies, reconstructing structural information. The final output is created by the elemental addition of the outputs of the two branches.

3.3 Train Loss

Our train loss consists of two parts, one is used to Train the cross-entropy loss of water type, and the other is image enhancement loss.

3.3.1 Cross-entropy loss

We calculate the cross entropy between the predicted water type and the target water type to train the classifier and improve the prediction accuracy. The cross-entropy loss is as follows:

$$L_C(I, C) = -\sum_{c=1}^{M} y_c log I_c \quad (5)$$

Here, I is the output of the classifier, C is the real water type and c is the classifier predicted water type. $y_c = 1$ if $C = c$, i.e., when the classifier predicts the correct water type, otherwise $y_c = 0$.

3.3.2 Reconstruction loss

To ensure that the rendering effect of the generated image is closer to ground truth, we propose an aggregation loss. The proposed reconstruction loss is defined as follows:

$$L_R(Y, Y_G) = \alpha L_{\mathrm{SSIM}}(Y, Y_G) + \beta L_{Color}(Y, Y_G) + \gamma L_{MSE}(Y, Y_G) \quad (6)$$

where α , β , γ represent the proportional coefficients of each loss component, we set them to 0.4, 0.4, and 0.2. L_{SSIM}, L_{Color} and L_{MSE} are describle as follows.

Structual similarity (SSIM) loss function is able to evaluate well the brightness, contrast and structure of the generated image, so it is used to learn both of high- and low-frequency information. The loss function is as follows:

$$L_{SSIM}(Y,Y_G) = 1 - \frac{(2\mu_Y\mu_{Y_G}+C_1)(\sigma_{YY_G}+C_2)}{(\mu_Y^2+\mu_{Y_G}^2+C_1)(\sigma_Y^2+\sigma_{Y_G}^2+C_2)} \quad (7)$$

Where Y is the enhancement image, Y_G is the ground truth image. μ_Y and σ_Y denote the enhanced result mean and standard deviation, μ_{Y_G} and σ_{Y_G} denote the ground truth mean and standard deviation. σ_{YY_G} is the covariance between the enhanced image and the ground truth. In this study, we set $C_1 = C_2 = 1e-5$, which is used to prevent the denominator from being zero.

Inspired by Muwei yet al. [8], we calculate the color difference of different channels between the lowfrequency feature image and ground truth, which is used to learn color information, the loss function is given as

$$L_{color}(Y,Y_G) = \|0.4\Delta R^2 + 0.4\Delta G^2 + 0.2\Delta B^2\|_2 \quad (8)$$

where ΔR, ΔG, ΔB represents the color difference between different channels in RGB color space.

MSE loss is used to calculate the reconstruction loss between the clear image and the enhanced image. It is defined as follows:

$$L_{MSE}(Y,Y_G) = \|Y - Y_G\|_2^2 \quad (9)$$

4. EXPERIMENT

Our model is implemented by the PyTorch framework on a Windows 10 workstation equipped with an NVIDIA GTX2070 GPU. We train the proposed model on real world dataset [4] and synthetic dataset [19] with a total of 10K pairs of underwater images and 300 epoches of training. We conduct extensive experiments in various dataset to explore the effectiveness of the proposed model. we compare the proposed model with several representative approach, including IBLA [17], UDCP [20], ULAP [21], RGHS [22], CycleGAN [23], SESR [3], DAL [5]. Besides, ablation studies are conducted to demonstrate the advantages of each component in our model.

We use two evaluation metrics, SSIM [24] and Peak Signal to Noise Ratio (PSNR) [25-27], to objectively assess the enhancement performance of the model. SSIM is defined as:

$$SSIM(Y,Y_G) = \frac{(2\mu_Y\mu_{Y_G}+C_1)(\sigma_{YY_G}+C_2)}{(\mu_Y^2+\mu_{Y_G}^2+C_1)(\sigma_Y^2+\sigma_{Y_G}^2+C_2)} \quad (10)$$

here, the means of each symbol in this formula are the same as in Eq. (7). The formula of PSNR is detailed as follows:

$$PSNR(Y,Y_G) = 10 \times log_{10}\frac{255^2}{E_{MS}(Y,Y_G)} \quad (11)$$

$$E_{MS}(Y,Y_G) = \frac{1}{mn}\sum_{i=0}^{m-1}\sum_{n=0}^{n-1}\|Y(i,j) - Y_G(i,j)\|^2 \quad (12)$$

where E_{MS} represents the mean square error between the enhanced image Y and clear image Y_G mean square error. Higher values of SSIM and PSNR indicate that the image quality is closer to the clear image.

4.1 Evaluation on Real-World Underwater Images

We evaluate the proposed network and other methods in underwater images from UIEB [4]. The enhancement results of different methods are shown in Fig. 2, which shows the comparison results of underwater images with different watercolor tones. According to the comparison results, our model has favorable visual perception, and independent of water type. Table 1 lists the PSNR and SSIM values of comparison methods. The proposed method has the most competitive results in these metrics, indicating that our method is effective, can deal with the effects of underwater image degradation caused by different water types.

Table 1. Underwater image quality evaluation of different variants of the presented method. Bold values show the best performer

Metric	Raw	UDCP	ULAP	RGHS	IBLA	CycleGAN	SESR	DAL	Ours
PSNR	16.54	12.47	15.60	18.81	15.81	21.25	17.22	16.47	25.00
SSIM	0.78	0.57	0.70	0.81	0.71	0.85	0.78	0.75	0.91

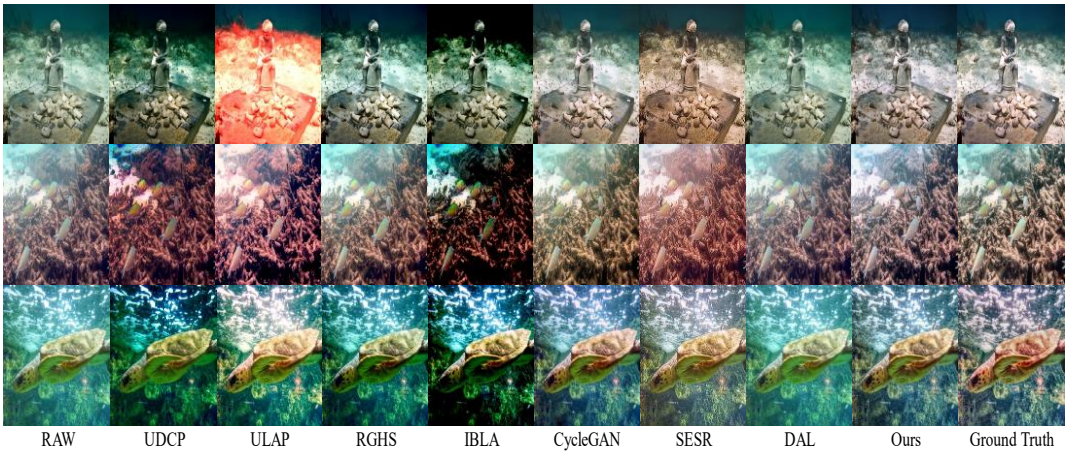

Fig. 2. Qualitative comparisons of results on real-world underwater images

Table 2. Underwater image quality evaluation of different variants of the presented method. The three rows of each dataset from top to bottom denote PSNR and SSIM scores, respectively. Bold values show the best performer

Dataset	Raw	UDCP	ULAP	RGHS	IBLA	CycleGAN	SESR	DAL	Ours
UFO	20.30	14.55	19.07	17.84	17.70	20.01	25.17	19.33	26.55
	0.77	0.57	0.73	0.74	0.65	0.82	0.83	0.76	0.84
SC	15.54	12.28	17.46	15.82	15.85	18.84	20.52	19.23	27.85
	0.73	0.54	0.73	0.72	0.65	0.78	0.79	0.77	0.87
IGN	20.91	14.34	19.83	18.30	18.58	19.85	25.67	19.35	28.31
	0.77	0.55	0.74	0.75	0.66	0.78	0.86	0.75	0.87

To further validate the generality of the model, we use the UFO-120 [8], EUVP-Imagenet [9] and EUVP-Scenes [9] datasets (denoted by UFO, IGN and SC, respectively) as test evaluations. The visual results are shown in Figure. 3, and the PSNR and SSIM values are shown in Table 2. Compared with other methods, the proposed method shows excellent performance in terms of contrast enhancement and detail recovery. Both quantitative and qualitative results are sufficient to show that our method has good perceptual properties with high quality recovery results, and the trained model is capable of good generalization performance.

4.2 Evaluation on Synthetic Underwater Images

In this experiment, we evaluate the performance of synthetic underwater images for different water types. Fig. 4 presents the visual comparison for different methods. Compared with other methods, the proposed method effectively enhances the visibility of multiple water types, restores relatively realistic colors and details in very low visibility, and the processing results of the model are visually closer to clear images. Table 3. lists the average values of PSNR and SSIM in the synthetic underwater data set for eight water types. These quantitative results show that our proposed network achieves satisfactory results.

4.3 Ablation Experiments

We performed ablation experiments on key components of the model in the UIEB underwater image dataset, and the visual comparison results are shown in Fig. 5. As shown in Fig. 5 (b), after removing the adaptive module, the watercolor effect is still present although the model improves the contrast to some extent. Significant edge sharpening and loss of detail can be observed after removing the high-frequency branch, as shown in Fig. 5 (b). As shown in Fig. 5 (c), after removing the low-frequency branch, enhancement result shows blurring and color shift. As shown in Fig. 5 (d), the results of the full model are closest to the ground truth. The average scores of PSNR and SSIM are presented in Table 4. These experiments validate the effectiveness of each component of the model.

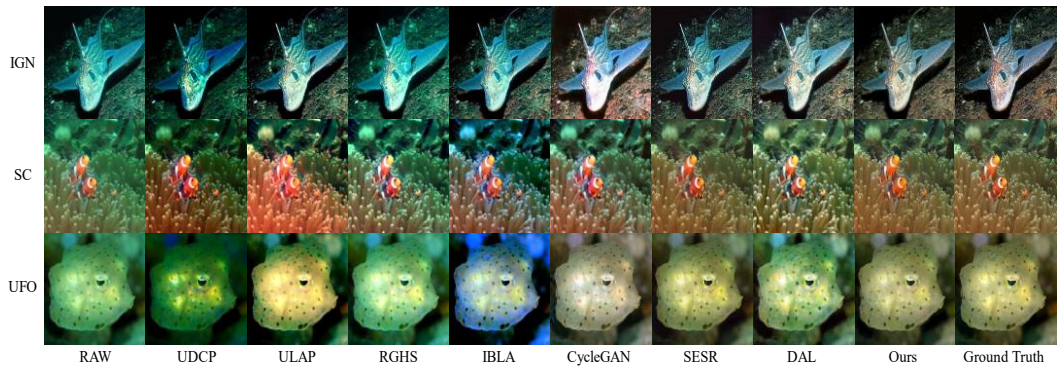

Fig. 3. Qualitative comparisons of results on test real-world underwater images

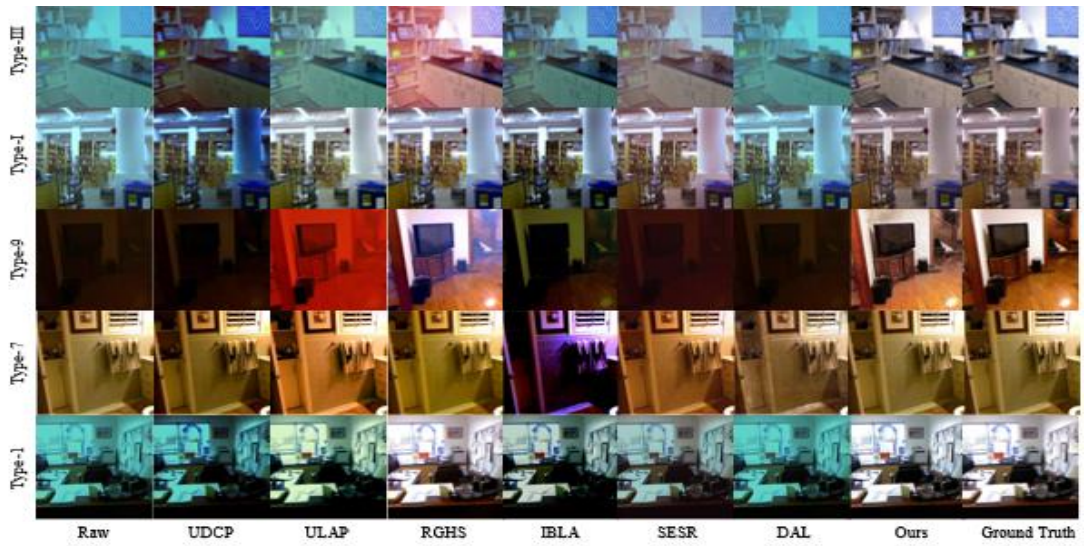

Fig. 4. Qualitative comparisons of results on synthetic underwater images

Table 3. Quantitative comparisons of results on synthetic underwater images. The two lower rows of each type denote PSNR and SSIM scores, respectively. Bold values show the best performer

Type	Raw	UDCP	ULAP	RGHS	IBLA	CycleGAN	SESR	DAL	Ours
Type-1	13.24	14.50	13.97	13.74	15.02	14.64	15.85	22.98	26.39
	0.68	0.70	0.69	0.74	0.68	0.65	0.70	0.82	0.90
Type-3	12.86	11.86	12.40	11.30	12.97	14.07	13.95	21.92	22.59
	0.62	0.61	0.60	0.66	0.63	0.64	0.60	0.78	0.85
Type-5	10.44	9.23	11.02	9.72	10.87	13.07	11.93	21.08	23.51
	0.48	0.42	0.53	0.59	0.50	0.63	0.45	0.73	0.82
Type-7	8.11	7.74	9.89	8.41	8.82	19.52	9.58	19.73	18.59
	0.28	0.22	0.42	0.51	0.30	0.59	0.30	0.66	0.67
Type-9	7.59	7.68	8.99	6.86	7.71	10.93	8.57	15.80	17.49
	0.19	0.18	0.29	0.44	0.18	0.45	0.22	0.58	0.59
Type-I	15.72	17.87	14.61	14.69	9.06	17.10	15.28	24.23	29.41
	0.81	0.83	0.76	0.78	0.20	0.74	0.75	0.85	0.94
Type-II	15.23	17.10	14.61	14.22	15.00	15.86	16.32	23.59	27.64
	0.79	0.81	0.76	0.76	0.65	0.73	0.74	0.84	0.93
Type-III	14.06	14.57	13.60	14.74	15.00	15.20	15.92	15.83	26.80
	0.72	0.73	0.70	0.75	0.77	0.68	0.71	0.75	0.91

Table 4. Ablation experiments for each key component. Bold values show the best performer

Metric	-AM	-HF branch	-LF branch	Full
PSNR	23.81	22.27	22.06	25.00
SSIM	0.90	0.88	0.90	0.91

(a) Raw (b) -AM (c) –HF Branch (d) -LF Branch (e) Ours (f) Ground Truth

Fig. 5. Ablation experiments for each key component

5. CONCLUSION

We propose a novel underwater image enhancement network that can adaptively handle the negative effects of different water types on the enhanced images, thus providing a generalized enhancement network. In addition, the proposed dual-layer synchronized enhancement network can learn the feature information of different frequencies underwater, which leads to a more realistic sensory effect of the enhanced image. Meanwhile, extensive experimental results on real underwater images and synthetic images with different water types show that the method is competitive and generalizable.

COMPETING INTERESTS

Authors have declared that no competing interests exist.

REFERENCES

1. Syed Waqas Zamir, Aditya Arora, Salman Khan, Munawar Hayat, Fahad Shahbaz Khan, Ming-Hsuan Yang. Restormer: Efficient transformer for high-resolution image restoration. In Proceedings of the IEEE/CVF Conference on Computer Vision and Pattern Recognition. 2022;5728–5739.
2. Adarsh Jamadandi and Uma Mudenagudi. Exemplar-based underwater image enhancement augmented by wavelet corrected transforms. In Proceedings of the IEEE/CVF Conference on Computer Vision and Pattern Recognition Workshops. 2019;11–17.
3. Md Jahidul Islam, Peigen Luo, Junaed Sattar. Simultaneous enhancement and super-resolution of underwater imagery for improved visual perception. ArXiv Preprint arXiv:2002.01155; 2020.
4. Chongyi Li, Chunle Guo, Wenqi Ren, Runmin Cong, Junhui Hou, Sam Kwong, and Dacheng Tao. An underwater image enhancement benchmark dataset and beyond. IEEE Transactions on Image Processing. 2019;29:4376–4389.
5. Pritish M Uplavikar, Zhenyu Wu, Zhangyang Wang. All-in-one underwater image enhancement using domain-adversarial learning. In CVPR Workshops. 2019;1–8.
6. Lintao Peng, Chunli Zhu, and Liheng Bian. U-shape transformer for underwater image enhancement. Arxiv preprint arXiv: 2111.11843; 2021.
7. Zhou J, Pang L, Zhang D, Zhang W. Underwater image enhancement method via multi-interval subhistogram perspective equalization, in IEEE Journal of Oceanic Engineering. 2023;48(2):474-488.
8. Muwei Jian, Xiangyu Liu, Hanjiang Luo, Xiangwei Lu, Hui Yu, and Junyu Dong. Underwater image processing and analysis: A review. Signal Processing: Image Communication, 2021;91:11608 8.
9. Chongyi Li, Saeed Anwar, Junhui Hou, Runmin Cong, Chunle Guo, Wenqi Ren. Underwater image enhancement via medium transmission-guided multi-color

space embedding. IEEE Transactions on Image Processing. 2021;30:4985–5000.
10. John Y Chiang, Ying-Ching Chen. Underwater image enhancement by wavelength compensation and dehazing. IEEE Transactions on Image Processing. 2011;21(4):1756– 1769.
11. Prasen Kumar Sharma, Ira Bisht, Arijit Sur. Wavelength-based attributed deep neural network for underwater image restoration. ACM Journal of the ACM (JACM); 2021.
12. Paul Drews, Erickson Nascimento, Filipe Moraes, Silvia Botelho, and Mario Campos. Transmission estimation in underwater single images. In Proceedings of the IEEE International Conference on Computer Vision Workshops. 2013;825–830.
13. Kaiming He, Jian Sun, Xiaoou Tang. Single image haze removal using dark channel prior. IEEE Transactions on Pattern Analysis and Machine Intelligence. 2010;33(12):2341–2353.
14. Saeed Anwar, Chongyi Li, and Fatih Porikli. Deep underwater image enhancement. Arxiv preprint arXiv:1807.03528; 2018.
15. Zhou J, Wang Y, Li C, Zhang W. Multicolor light attenuation modeling for underwater image restoration, in IEEE Journal of Oceanic Engineering. 2023;48(4):1322-1337.
16. Hou G, Li N, Zhuang P, Li K, Sun H, Li C. Non-Uniform Illumination Underwater Image Restoration via Illumination Channel Sparsity Prior. in IEEE Transactions on Circuits and Systems for Video Technology. 2024;34(2):799-814.
17. Nils Gunnar Jerlov. Marine optics. Elsevier; 1976.
18. Pan Z, Cai J, Zhuang B, Fast vision transformers with hilo attention, in NeurIPS; 2022.
19. Peng YT, Cosman PC. Underwater image restoration based on image blurriness and light absorption. IEEE Trans Image Process. 2017;26(4):1579–1594.
20. Paulo LJ Drews, Erickson R Nascimento, Silvia SC Botelho, and Mario Fernando Montenegro Campos. Underwater depth estimation and image restoration based on single images. IEEE Computer Graphics and Applications. 2016;36(2):24–35, 2016.
21. Wei Song, Yan Wang, Dongmei Huang, Dian Tjondronegoro. A rapid scene depth estimation model based on underwater light attenuation prior for underwater image restoration. In Pacific Rim Conference on Multimedia. Springer. 2018;678–688.
22. Dongmei Huang, Yan Wang, Wei Song, Jean Sequeira, Sébastien Mavromatis. Shallow-water image enhancement using relative global histogram stretching based on adaptive parameter acquisition. In International conference on multimedia modeling, pages. Springer. 2018;453–465.
23. Jun-Yan Zhu, Taesung Park, Phillip Isola, Alexei A Efros. Unpaired image-toimage translation using cycle-consistent adversarial networks. In Proceedings of the IEEE International Conference on Computer Vision Pages. 2017;2223–2232.
24. Wang Zhou et al. Image quality assessment: From error visibility to structural similarity, IEEE Transactions on Image Processing. 2004;13(4):600–612.
25. Korhonen Jari, Junyong You. Peak signal-to-noise ratio revisited: Is simple beautiful? Proceedings of the 2012 Fourth International Workshop on Quality of Multimedia Experience. 2012;38–38.
26. Md Jahidul Islam, Sadman Sakib Enan, Peigen Luo, and Junaed Sattar. Underwater image super-resolution using deep residual multipliers. In 2020 IEEE International Conference on Robotics and Automation (ICRA). IEEE, 2020;900–906.
27. Md Jahidul Islam, Youya Xia, Junaed Sattar. Fast underwater image enhancement for improved visual perception. IEEE Robotics and Automation Letters. 2020;5(2):3227–3234.

Peer-review history:
The peer review history for this paper can be accessed here:
https://www.sdiarticle5.com/review-history/115216